



Pergamon

Materials Research Bulletin 36 (2001) 2183–2198

Materials  
Research  
Bulletin

## Effect of the atomic size distribution on glass forming ability of amorphous metallic alloys

O.N. Senkov<sup>\*,a</sup>, D.B. Miracle<sup>b</sup>

<sup>a</sup>*Air Force Research Laboratory, Materials and Manufacturing Directorate, Wright-Patterson AFB, OH 45433-7817, USA,*

<sup>b</sup>*UES Inc., 4401 Dayton-Xenia Rd., Dayton, OH 45432-1894, USA*

(Refereed)

Received 10 March 2001; accepted 11 June 2001

---

### Abstract

A topological approach based on analysis of atomic size distributions has been developed and applied to multicomponent amorphous alloys with different glass-forming ability. The atomic size distributions were obtained by plotting atomic concentrations versus atomic radii of constitutive elements. Ordinary amorphous alloys with high critical cooling rates were found to have single-peak distributions with a concave downward shape. These amorphous systems have at least one alloying element with a smaller radius, and at least one alloying element with a larger radius relative to the base element. The concentration of an alloying element decreases rapidly as the difference in the atomic sizes of the base element and the alloying element increases. Atomic size distributions of Zr, Pd, or Ln-based bulk amorphous alloys, which have a critical cooling rate in the range of 1–100 K/s, have a completely different, concave upward shape with a minimum at an intermediate atomic size. The base alloying element in these alloys has the largest atomic size and the smallest atom often has the next-highest concentration. A model that explains the concave upward shape of atomic size distributions for the bulk amorphous alloys is suggested. This model takes into account that all alloying elements in bulk glass formers are smaller than the matrix element, and some of them are located in interstitial sites while others substitute for matrix atoms in a reference crystalline solid solution. The interstitial and substitutional atoms attract each other and produce short-range ordered atomic configurations that stabilize the amorphous state. According to this model, the critical concentration of an interstitial element required to amorphize the alloy increases with increasing size difference from the matrix atom. © 2001 Elsevier Science Ltd. All rights reserved.

*Keywords:* A. Amorphous materials; A. Metals

---

\* Corresponding author.

*E-mail address:* oleg.senkov@wpafb.af.mil (O.N. Senkov).

## 1. Introduction

Amorphous metallic alloys have unique mechanical and physical properties attributed to the atomic structure of the amorphous phase. Generally, high cooling rates, above  $10^5$  K/s, are required to produce amorphous alloys in the form of ribbons, flakes, or powders, with the resulting sample thickness less than 50  $\mu\text{m}$  [1], and great efforts have been made to consolidate this material into a bulk amorphous part. Recently, new multicomponent alloy systems with much lower critical cooling rates ( $\leq 10^2$  K/s) have been developed, which can produce fully amorphous products by a conventional casting process to a thickness as large as about 100 mm [2–4]. Most of these bulk amorphous alloys contain very expensive elements of platinum and/or lanthanum groups limiting their applications, and only Zr-based alloys that do not contain these elements have found successful use for sporting goods [3].

Since the discovery of amorphous alloys, a number of attempts have been made to understand the mechanism of amorphization in order to predict alloy compositions with better glass-forming ability. Three empirical rules have been defined for the bulk amorphous alloy systems [4]. These are (a) requirement of three or more elements; (b) significant difference in atomic size ratios above about 12% among the three main constituent elements; and (c) negative heats of mixing among the three main constituent elements. The glass formation composition range generally coincides with an eutectic region, and a reduced glass transition temperature,  $T_{rg} = T_g/T_m$ , as high as 0.6–0.7 is typical for easy glass formers [5]. ( $T_m$  is the liquidus temperature and  $T_g$  is the glass transition temperature.) The density difference between the amorphous and fully crystalline states for bulk amorphous alloys is in the range of 0.3–0.54%, which is much smaller than the values of about 2% for ordinary amorphous alloys [6]. This indicates that bulk amorphous alloys have higher dense randomly packed atomic configurations than ordinary amorphous alloys. Formation of the liquid with specific atomic configurations and multicomponent interactions on a short-range scale has been suggested to increase the solid/liquid interfacial energy and decrease atomic diffusivity, which in turn, leads to suppression of nucleation and growth of crystalline phases [4]. Topological complexity and frustration was given in ref. [3] as another explanation of suppression of crystallization in the multicomponent alloys.

Although these empirical rules give useful directions, these are rather general, and the development of new amorphous alloys is still a very time-consuming process of selection and screening of different element combinations that is guided by empirical rather than scientific considerations. Finding more specific criteria for easy glass-forming alloy systems would, therefore, be beneficial. In the present work, some topological features of ordinary and bulk amorphous alloys are considered and discussed, which might be useful in the selection of alloy compositions for prospective bulk amorphous materials.

In his early work, Bernal suggested that the structure of a liquid is determined by volume exclusion [7]. He proposed a model in which the atoms were considered as hard spheres, and their local structure determined by the restrictions on space-filling sequent upon the inability of two atoms to approach more closely than one diameter. This single component model predicts the maximum random packing density of the melt to be 0.664 [8]. If this value is compared with the maximum packing density of a crystalline phase (0.74 for fcc or hcp structures), the model predicts the volume expansion at the melting temperature of about

11.4%, which is higher than the experimentally observed 2–10% expansion range for pure metals [9,10]. The model would agree with the experiment only if the metals crystallize in less dense crystal structures such as the body centered cubic (bcc, the packing density = 0.68). In the latter case, the volume expansion predicted from the model is 6.25%. Additional improvements in the model can give better agreement with the experiment; however, it is clear that the volume expansion of pure metals at melting (about 6% [10]) is much higher than that of amorphous alloys (2% or less). The small difference in the volume expansion of amorphous alloys can be due to two reasons: (1) the random packing density of atoms in these multicomponent alloys is higher than in the single-component pure metals, and/or (2) the packing density of these alloys in the fully crystallized state is low. Taking into account that the metallic alloys tend to form high density crystalline lattices [11], one can assume that the first reason is the most significant.

It is known from powder metallurgy that the random packing density can be increased if particles of different sizes are present in the material in a certain proportion [12]. One may, therefore, assume that a similar situation occurs in multicomponent alloys: the random dense packing of a certain proportion of smaller and larger atoms decreases the mean size of interatomic voids and increases the density of the amorphous phase. It may, therefore, prove valuable to analyze the atomic size distributions in different amorphous alloys. In the present article, more than 100 alloys containing at least three elements were analyzed. The compositions were taken from refs. [1–3,15,16]. Binary amorphous alloys are not described in this work, because bulk amorphous materials are not produced from binary alloys. The atomic size effect on the formability of many binary metallic glasses has already been analyzed elsewhere [13,14].

## 2. Atomic Size Distributions for Ordinary Amorphous Alloys

To obtain the atomic size distribution for an amorphous alloy, atomic concentrations were plotted versus atomic radii of the constitutive elements. The radii used in this study were obtained by a critical assessment of data in the literature [21–23], and are shown in Table I. These values are for first-order comparisons only, as the actual atom radii depend upon the structure and local chemical environment, and significantly smaller or larger radii may result, depending upon neighbor with which a bond is formed. For example, significant bond shortening is observed in the Fe–Al system [14]. Nonetheless, the data provides a consistent basis for comparison and discussion. Atoms with  $\leq 2\%$  size difference were counted as one group of atoms in these distributions. Representative examples of the atomic size distributions typical to most ordinary (not bulk) amorphous alloys [based on Fe, Ni, ( $\text{Fe}_x\text{Ni}_{1-x}$ ), Co, Cr, Cu, or Al], for which the critical cooling rate is about  $10^4$ – $10^6$  K/s, are shown in Fig. 1. Representative metal/metalloid systems are shown in Fig. 1a and b, and metal/metal systems are shown in Fig. 1c. The distributions have a single peak that occurs at the atomic radius corresponding to the base element. These amorphous systems have at least one alloying element with a smaller radius and at least one alloying element with a larger radius relative to the base element. The concentration of an alloying element depends on its atomic radius, decreasing rapidly as the difference in the atomic sizes of the base element and the

Table 1

Atomic radii of different elements used in the current work to plot atomic size distributions for a number of amorphous alloys

Element	Symbol	Atomic No.	Radius (nm)	Source
Oxygen	O	8	0.07300	[21]
Nitrogen	N	7	0.07500	[21]
Carbon	C	6	0.07730	[21]
Boron	B	5	0.08200	[21]
Sulfur	S	16	0.10200	[21]
Phosphorus	P	15	0.10600	[22]
Beryllium	Be	4	0.11280	[23]
Silicon	Si	14	0.11530	[22]
Germanium	Ge	32	0.12400	[22]
Iron	Fe	26	0.12412	[23]
Nickel	Ni	28	0.12459	[23]
Chromium	Cr	24	0.12491	[23]
Cobalt	Co	27	0.12510	[23]
Copper	Cu	29	0.12780	[23]
Vanadium	V	23	0.13160	[23]
Ruthenium	Ru	44	0.13384	[23]
Rhodium	Rh	45	0.13450	[23]
Manganese	Mn	25	0.13500	[21]
Osmium	Os	76	0.13523	[23]
Iridium	Ir	77	0.13573	[23]
Technetium	Tc	43	0.13600	[23]
Molybdenum	Mo	42	0.13626	[23]
Tungsten	W	74	0.13670	[23]
Rhenium	Re	75	0.13750	[23]
Palladium	Pd	46	0.13754	[23]
Platinum	Pt	78	0.13870	[23]
Gallium	Ga	31	0.13920	[22]
Zinc	Zn	30	0.13945	[23]
Selenium	Se	34	0.14000	[21]
Uranium	U	92	0.14200	[21]
Niobium	Nb	41	0.14290	[23]
Tantalum	Ta	73	0.14300	[23]
Aluminum	Al	13	0.14317	[23]
Gold	Au	79	0.14420	[23]
Silver	Ag	47	0.14447	[23]
Tellurium	Te	52	0.14520	[22]
Titanium	Ti	22	0.14615	[23]
Lithium	Li	3	0.15194	[23]
Polonium	Po	84	0.15300	[21]
Thulium	Tm	69	0.15600	[21]
Cadmium	Cd	48	0.15683	[23]
Hafnium	Hf	72	0.15775	[23]
Magnesium	Mg	12	0.16013	[23]
Zirconium	Zr	40	0.16025	[23]
Protactinium	Pa	91	0.16100	[21]
Tin	Sn	50	0.16200	[21]
Promethium	Pm	61	0.16300	[21]
Neodymium	Nd	60	0.16400	[21]
Scandium	Sc	21	0.16410	[23]
Praseodymium	Pr	59	0.16500	[21]
Indium	In	49	0.16590	[22]

Table 1  
(Continued)

Element	Symbol	Atomic No.	Radius (nm)	Source
Ytterbium	Yb	70	0.17000	[21]
Thallium	Tl	81	0.17160	[23]
Lutetium	Lu	71	0.17349	[23]
Lead	Pb	82	0.17497	[23]
Erbium	Er	68	0.17558	[23]
Holmium	Ho	67	0.17661	[23]
Dysprosium	Dy	66	0.17740	[23]
Terbium	Tb	65	0.17814	[23]
Thorium	Th	90	0.18000	[23]
Gadolinium	Gd	64	0.18013	[23]
Yttrium	Y	39	0.18015	[23]
Samarium	Sm	62	0.18100	[21]
Cerium	Ce	58	0.18247	[23]
Sodium	Na	11	0.18570	[23]
Lanthanum	La	57	0.18790	[23]
Calcium	Ca	20	0.19760	[23]
Europium	Eu	63	0.19844	[23]
Strontium	Sr	38	0.21520	[23]
Barium	Ba	56	0.21760	[23]
Potassium	K	19	0.23100	[23]
Rubidium	Rb	37	0.24400	[23]
Cesium	Cs	55	0.26500	[23]

alloying element increases. This empirical observation is consistent with the criterion developed by Egami for binary amorphous alloys [10,13,14].

### 3. Atomic Size Distributions for Bulk Amorphous Alloys

Fig. 2 shows the atomic size distributions for Mg and Cu-based bulk amorphous alloys. The critical cooling rates for the Mg-based alloys are 30–100 K/s and for Cu-based alloys are  $\sim 10^2$ – $10^3$  K/s [4]. The distributions have a concave downward shape, similar to ordinary amorphous alloys; however, the peaks are asymmetrical relative to the maximum.

Figure 3 shows the atomic size distributions typical for the Fe and Co-based bulk amorphous alloys. The distributions differ from those for ordinary alloys by the presence of valleys on both sides of the peak.

Pd-based alloys that have relatively low critical cooling rates for amorphization, about 10–500 K/s, have atomic size distributions shown in Fig. 4. The base alloying element has the largest atomic size in these systems, and the concentrations of other alloying elements decrease when the atomic size decreases or show a minimum at an intermediate atomic size. Platinum and rare-earth metal (Ln)-based amorphous alloys also have similar distributions (Fig. 5).

Fig. 6 shows the atomic size distributions for several Zr-based bulk amorphous alloys, which have a critical cooling rate in the range of 1–500 K/s. Two characteristic distributions can be distinguished. The alloys with higher critical cooling rates have atomic size distri-

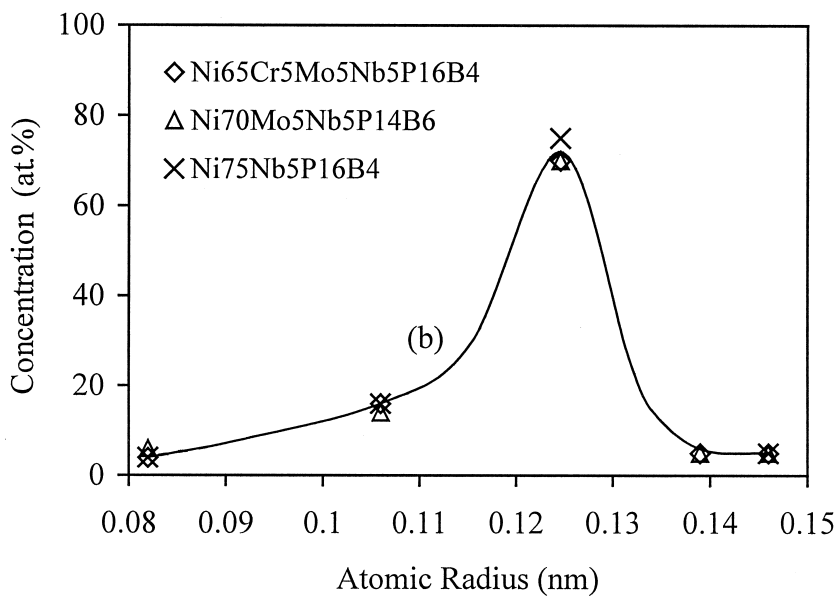
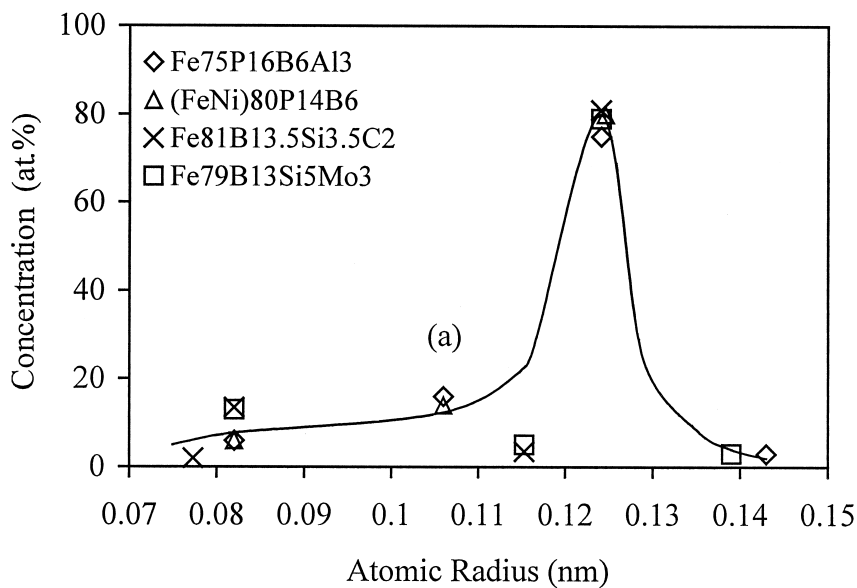


Fig. 1. Atomic size distributions in several (a) Fe, (b) Ni, and (c) Al-based ordinary amorphous alloys. Critical cooling rates are  $\sim 10^4$ – $10^6$  K/s.

butions with two peaks, corresponding to Cu and Zr atoms, and a minimum between the peaks (Fig. 6a), while the alloys that show the best glass-forming ability have a concave upward shape (Fig. 6b), similar to Pd-based alloys. In these latter alloys, the base alloy

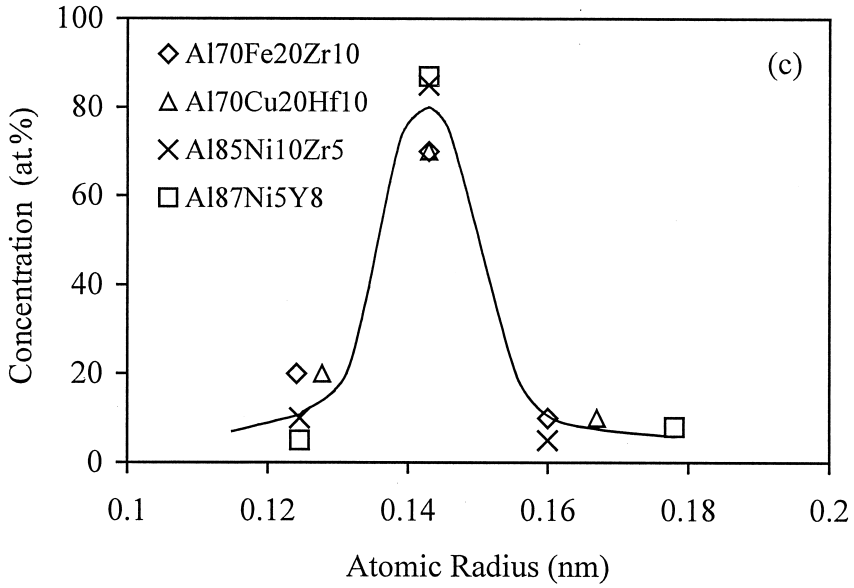


Fig. 1. (Continued)

element (that is the element with the highest atomic concentration) is the largest atom and the smallest atom often has the next-highest concentration, while atoms of intermediate radii are generally present at the lowest concentrations. Thus, a concave upward plot generally characterizes bulk amorphous alloys with very good glass forming ability.

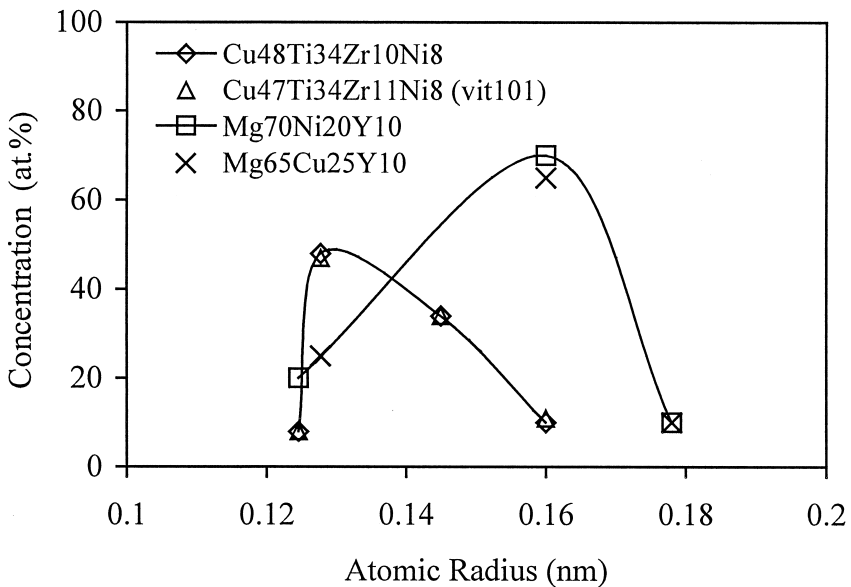


Fig. 2. Atomic size distributions in several Mg- and Cu-based bulk amorphous alloys. Critical cooling rates are ~30–1000 K/s.

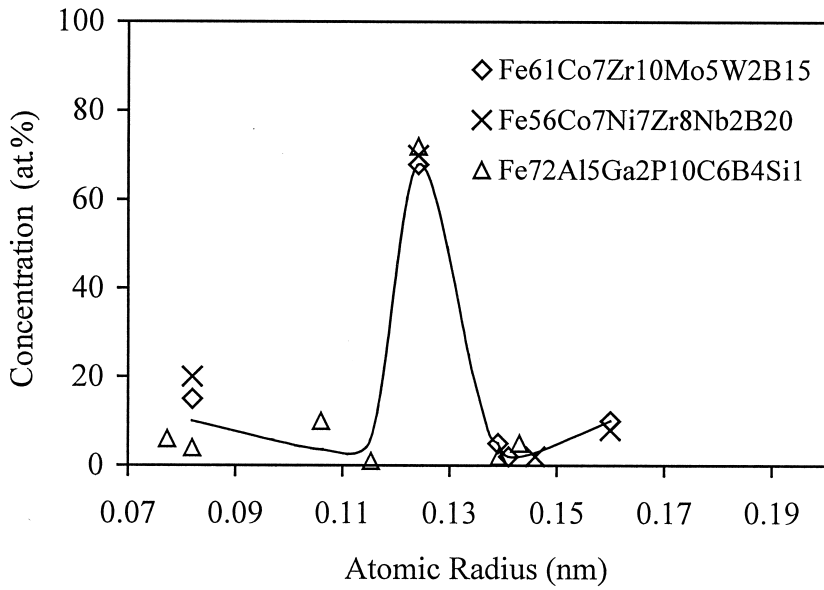


Fig. 3. Atomic size distributions in several Fe-based bulk amorphous alloys. Critical cooling rates are  $\sim 10^2$ – $10^4$  K/s.

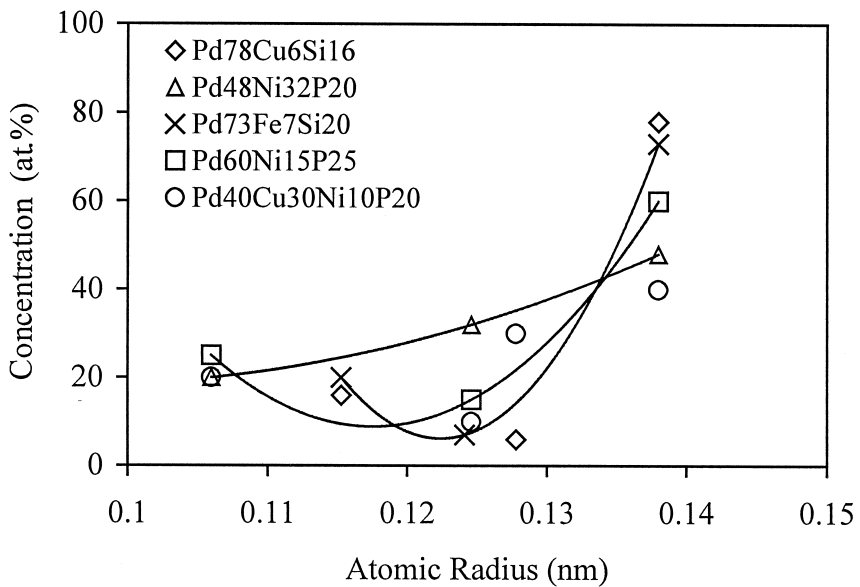


Fig. 4. Atomic size distributions in several Pd-based bulk amorphous alloys. Critical cooling rates are  $\sim 10$ – $500$  K/s.

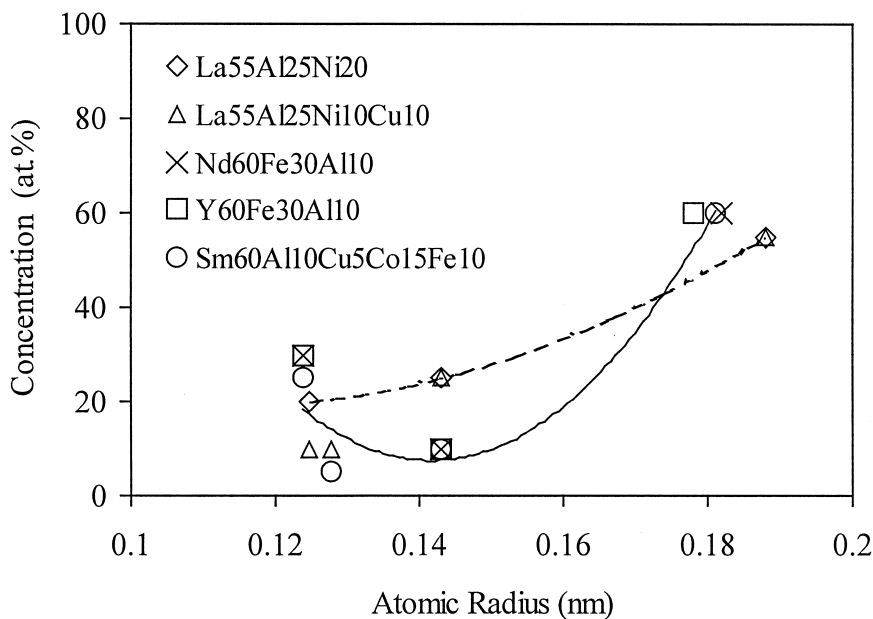


Fig. 5. Atomic size distributions in several Ln-based bulk amorphous alloys. Critical cooling rates are  $\sim 10$ – $1000$  K/s.

#### 4. Discussion

Valuable insight is gained from analysis of the restricted compositional range over which an amorphous structure is obtained. The composition of glass-forming alloys is used to obtain specific information relating to the two most important topological parameters—the atomic sizes (from the types of atoms present) and relative numbers of atoms. Using this information, atomic size distributions (composition versus atomic radius curves) are plotted for a number of amorphous alloys with different glass-forming ability (GFA) and a difference is distinguished between alloys with marginal GFA (that is alloys with a critical cooling rate greater than  $\sim 10^3$  K/s) and bulk metallic glasses (the critical cooling rate is less than  $10^3$  K/s).

Common trends are observed for amorphous alloys that have a critical cooling rate  $\geq 10^3$  K/s, Fig. 1. A typical formulation of these alloys is a ternary or higher order alloys with 60–90% of the base metal. A significant concentration of each alloying element ( $\geq 5\%$ ) is typical. At least one alloying element is smaller and at least one is larger than the base element, the atomic radius of at least one of them falls well outside a bound of 15% of the radius of the base atom, and the overall shape of the composition–radius plot is concave downward, with few exceptions.

The atomic size distribution transforms from a concave downward shape to a concave upward shape when the critical cooling rate decreases below  $\sim 10^2$ – $10^3$  K/s. For example, the Zr-, Pd-, and Ln-based bulk amorphous alloys, which are the best current glass formers, have concave upward-shape atomic size distributions, Figs. 4–6. This observation, along with the earlier observation that bulk glass-forming alloys have a higher relative density, lead

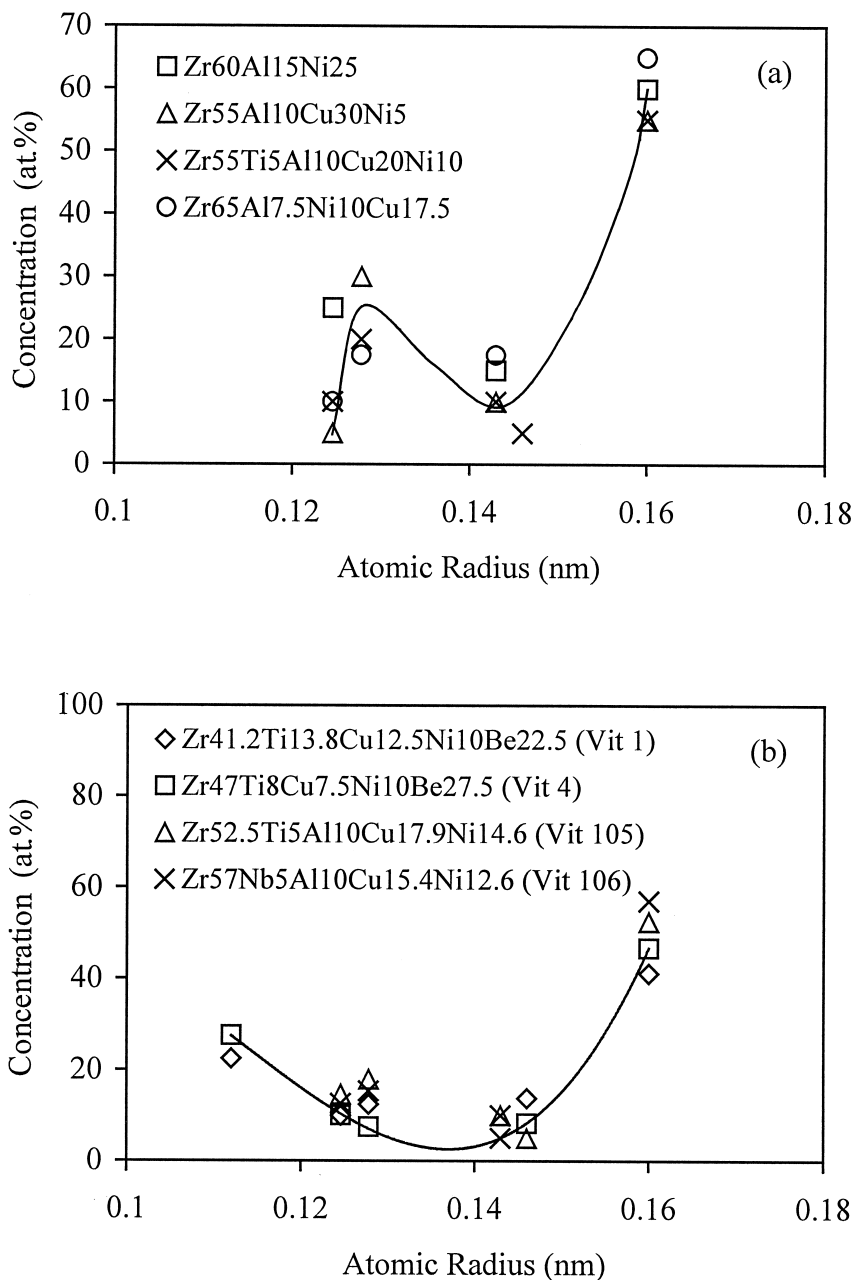


Fig. 6. Atomic size distributions in several Zr-based bulk amorphous alloys. Critical cooling rates are  $\sim 1$ –500 K/s.

to the conclusion that the concave upward distributions provide for more efficient atomic packing relative to alloys with a concave downward distributions. A more compact structure has been shown to have a higher viscosity and lower diffusivity, leading to a considerable decrease in atomic diffusion and the nucleation and growth of crystalline phases, and thus

strongly enhances bulk glass formability [17,18]. Additional studies will be required to specify why a concave upward distribution correlates so strongly with improved glass forming ability. There are a few exceptions from this trend, such as some Cu- and Mg-based alloys, and additional studies are also required to understand these deviations.

In their early work, Egami and Waseda [13] found a correlation between the glass formability and the extent of atomic size mismatch of the constituent atoms in a number of binary alloys:

$$C_{\min} = 0.1/|(R_B/R_A)^3 - 1| \quad (1)$$

In (1),  $R_A$  and  $R_B$  are radii of a host atom A and a solute atom B, respectively. The proportionality between the minimum concentration of a solute element,  $C_{\min}$ , needed to amorphise the matrix and the inverse of the reduced atomic volume difference  $(V_B - V_A)/V_A \equiv [(R_B/R_A)^3 - 1]$  was explained in terms of the instability of a crystalline solid solution generated by the atomic size difference. It was, therefore, assumed that amorphization (by rapid quenching or solid state reaction) can occur only when the crystalline solid solution is thermodynamically less stable than the undercooled melt. It was later suggested that a topological instability of a crystal lattice occurs when a certain (critical) level of internal stress is reached, leading to a reduced (or increased) coordination number [10,14]. Because only certain coordination numbers are allowed in crystals while more topological freedom is allowed in glasses, this topological transformation leads to amorphization and relaxes the internal stresses significantly [14,20].

The relation (1) was derived in a supposition that the alloying elements substitute for the matrix atoms at a regular lattice site. In this case, the concentration of the alloying element required to destabilize the crystal lattice decreases as the difference in atomic size between the matrix and alloying element increases, because a larger strain is introduced per atom for smaller substitutional atoms. The minimum concentrations derived from Eq. 1 are plotted as dashed lines in Fig. 7a and b for Al-based and Fe-based amorphous alloys. The atomic radii have been normalized by the radius of the base (Al or Fe) atom. Although it describes the general shape of the ordinary amorphous alloy distributions qualitatively well, this theory predicts much higher critical concentrations of alloying elements in these multicomponent alloys than experimentally obtained; this has already been mentioned elsewhere [20]. The discrepancy would be even higher if it were acknowledged that the smaller substitutional atoms should decrease the internal strains produced by the larger substitution atoms. Therefore, according to the Egami and Waseda criterion, much higher concentrations of smaller or larger atoms would be required to produce a topological instability in these multicomponent alloys. (Here, the terms ‘smaller’ and ‘larger’ refer relative to the size of the main matrix atom.)

It is necessary to point out that ordinary multicomponent amorphous alloys, which contain at least one larger alloying element and at least one smaller alloying element (see Fig. 1), are generally more stable than the binary amorphous alloys. This feature may be important for stabilization of the amorphous structure. Indeed, as substitutional atoms, the smaller atoms produce compressive lattice strains and the larger atoms produce tensile strains in the matrix. The opposite strain fields of the larger and smaller atoms should attract each other, thereby

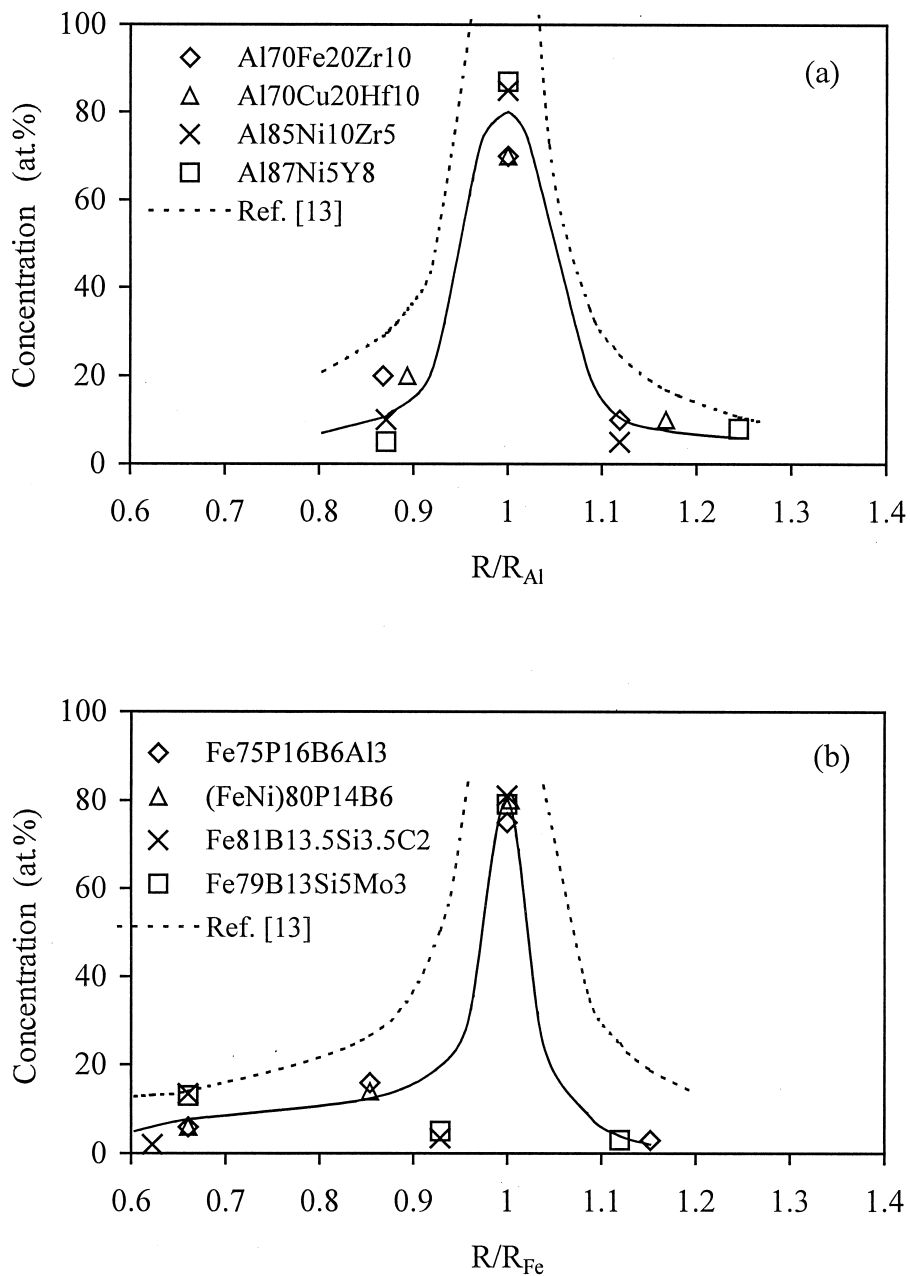


Fig. 7. Normalized atomic radius versus composition diagrams of ordinary (a) Al-based amorphous alloys and (b) Fe-based amorphous alloys. The dashed lines represent the minimum predicted concentrations required to destabilize the crystal lattice in binary alloys, from ref. [13].

reducing the internal stresses and forming relatively stable short-range ordered configurations (clusters). If these clusters are allowed by the crystal symmetry, their formation will stabilize the crystal and make amorphization more difficult. However, if the short-range

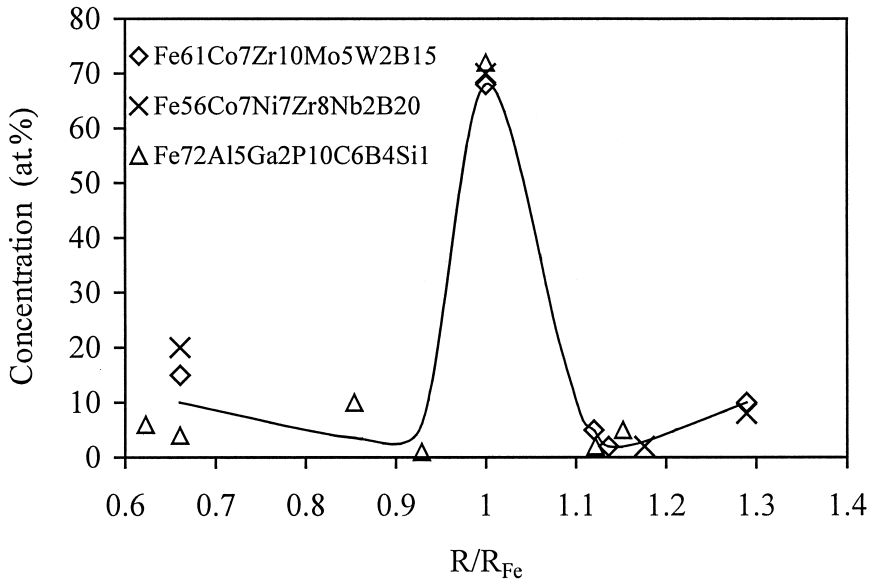


Fig. 8. Normalized atomic radius versus composition diagrams of bulk Fe-based amorphous alloys.

ordered clusters are not supported by the crystal symmetry of the solid solution, their formation should favor amorphization. Comparison of normalized atomic size distributions of ordinary (Fig. 7) and bulk (Fig. 8) Fe-based amorphous alloys shows that the latter alloys have larger amount of smaller (B, C) and/or larger (Al, Zr) elements; this probably increases in the degree of dense packing [4].

A critical feature is expected for alloy elements with a radius between about (0.6–0.85)  $R_A$ . Solute atoms with  $R_B > 0.6R_A$  produce a large tensile lattice strain in the octahedral site, while a large compressive lattice strain is produced for a substitutional site when  $R_B < 0.85R_A$ . However, no other lattice sites are available for solute atoms in this size range, so it is likely that atoms in this size range partition between these two sites. For example, Be and Ni atoms are, respectively, 29.5 and 22.1% smaller than a Zr atom, and a Ni atom is 33.7% smaller than an La atom, and these small atoms can be located in interstices between the large atoms, providing some distortions. The distortions decrease if the size difference between the matrix and interstitial atoms increases, which is opposite to the case of substitutional atoms. This may be a key for understanding why many bulk amorphous alloys have concave upward-type atomic size distributions. Indeed, a higher concentration of an interstitial atom is required to reach a critical internal stress for destabilization of the crystal lattice (amorphization) when the atomic size of this atom decreases relative to the size of the matrix atom; this is opposite to the situation with substitutional atoms. Producing tensile strains, these interstitial atoms would attract the substitution atoms that are smaller than the matrix atoms and repulse the substitutional atoms that are larger than the matrix atoms. In the former case, dense and stable short-range order atomic configurations may be produced, which may stabilize the amorphous state, while the latter case explains why bulk metallic glasses containing large amount of interstitial elements do not generally contain solute

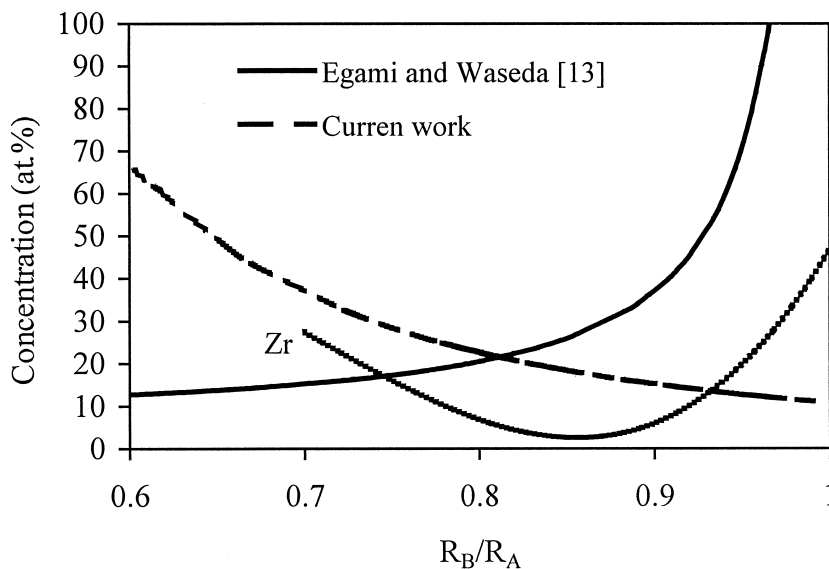


Fig. 9. Minimum concentrations of substitutional atoms (solid line) and interstitial atoms (dashed line) required for amorphization. A compositional curve for a bulk Zr-based alloy is also plotted as a dotted line.

elements with atomic sizes larger than the atomic size of the base element. It should also be noted that an alloying element with a size smaller than the matrix atom can occupy both interstitial and substitutional sites and produce attractive short-range order complexes. A smaller atomic size of an alloying element will lead to a higher fraction of the element in the interstitial sites to destabilize the crystal lattice.

An important role of interstitial atoms in destabilizing the crystalline phase has recently been suggested by Granato [19]. He developed an interstitialcy theory of melting where he showed that an increased concentration of interstitials should produce a dramatic softening of the shear modulus and a decrease in melting temperature; and at a critical concentration the melting transformation changes from first order to second order. At this critical point, the defective crystal becomes absolutely unstable and undergoes a continuous transformation to the supercooled liquid (frozen glassy state).

One may estimate the critical concentration of an interstitial element using an approach similar to that in ref. [13]; however, the radius of an interstitial site,  $R_I$ , should be used instead of the radius of the matrix atom,  $R_A$ . It is known that  $R_I$  is proportional to  $R_A$ , and the proportionality coefficient,  $K$ , depends on the type of interstitial site and the matrix structure. For example, for the octahedral site in the closed-packed structure,  $K = 0.4142$ . The critical concentration of an interstitial atom of radius  $R_B$  is then determined as:

$$C_i \cong 0.1R_A^3/|R_B^3 - K^3R_A^3| \quad (2)$$

The value of  $C_i$  determined from Eq. 2 is plotted in Fig. 9 as a dashed line versus  $R_B/R_A$ . The minimum concentration of substitutional atoms, according to Egami and Waseda criterion, is also shown in this figure. This interstitial model provides two important improvements over the Egami-Waseda model. First, it provides a basis for considering the influence of

ternary alloy additions on destabilization of a crystalline lattice. Second, it provides a physical basis for obtaining an increasing critical minimum concentration with increasing size difference from the host atom. This feature is required to understand the basis for bulk glass-forming alloys, and was not provided by previous models. In addition, the minimum solute concentration from this interstitial model, along with the earlier model for substitutional solutes, provides an approach for representing the concave upward plots of multicomponent bulk metallic glasses.

## 5. Conclusions

A method relating to the two most important topological parameters—the atomic sizes of the alloying elements and the relative numbers of atoms is proposed for visualizing common trends in amorphous metallic alloys with different glass forming abilities. In this method, each alloying element in an alloy provides a data point where the atomic size is plotted versus elemental concentration. Together, the data points from all of the elements in a particular alloy define a single curve—the atomic size distribution. The shapes of these composition–atomic radius curves are shown to distinguish between ordinary amorphous alloys with marginal GFA (that is, alloys with the critical cooling rate greater than  $\sim 10^3$  K/s), and bulk metallic glasses (for which the critical cooling rate is less than  $10^3$  K/s).

Ordinary amorphous alloys are found to have single-peak distributions with concave downward shape. These amorphous systems have at least one alloying element with a smaller radius and at least one alloying element with a larger radius relative to the base element. The concentration of an alloying element decreases rapidly as the difference in the atomic sizes of the base element and the alloying element increases. Atomic size distributions of many bulk metallic glasses have a completely different, concave upward shape with a minimum at an intermediate atomic size. The base alloying element in these alloys has the largest atomic size and the smallest atom often has the next-highest concentration.

A model that explains the concave upward shape of atomic size distributions for the bulk amorphous alloys is suggested. This model takes into account that all alloying elements in bulk glass formers are smaller than the matrix element, and some of them are located in interstitial sites while others substitute matrix atoms. The interstitial and substitutional atoms attract each other and produce short-range order atomic clusters that may stabilize the amorphous state. According to this model, the critical concentration of an alloying element required to amorphize the alloy decreases, approaches a minimum and then increases when the size ratio between the alloying element and the matrix atom decreases.

## Acknowledgments

The authors are indebted to Dr. G.J. Shiflet and Dr. S.J. Poon for discussion of the results and critical comments. The work was supported by the Air Force Research Laboratory, contract No. F33615-96-C-5258.

## References

- [1] F.E. Luborsky, (Ed.), *Amorphous Metallic Alloys*, Butterworths, London, 1983.
- [2] A. Inoue, *Prog. Mater. Sci.* 43 (1998) 365.
- [3] W.L. Johnson, in: W.L. Johnson, A. Inoue, C.T. Liu (Eds.), *Bulk Metallic Glasses*, MRS Symposium Proceedings, Vol. 554, Materials Research Society, Warrendale, PA, 1999, p. 311.
- [4] A. Inoue, *Acta Mater.* 48 (2000) 279.
- [5] H.A. Davies, in: F.E. Luborsky (Ed.), *Amorphous Metallic Alloys*, Butterworths, London, 1983, p. 8.
- [6] T. Matsumoto, (Ed.), *Materials Science of Amorphous Alloys*, Ohmu, Tokyo, 1983.
- [7] J.D. Bernal, *Proc. R. Soc. A*284 (1964) 299.
- [8] J.L. Finney, *Nature* 266 (1977) 309.
- [9] Y.S. Touloukian et al., (Eds.), *Thermophysical Properties of Matter*, vol. 12, Plenum, New York, 1979.
- [10] T. Egami, *Mater. Sci. Eng.* A226–A228 (1997) 261.
- [11] R.C. Evans, *Crystal Chemistry*, Cambridge Univ. Press, New York, 1964.
- [12] J.S. Reed, *Introduction to the Principles of Ceramic Processing*, John Wiley & Sons, New York, 1988, p. 185.
- [13] T. Egami, Y. Waseda, *J. Non-Cryst. Solids* 64 (1984) 113.
- [14] T. Egami, *J. Non-Cryst. Solids* 205–207 (1996) 575.
- [15] T.R. Anantharaman, *Metallic Glasses: Production, Properties and Applications*, Trans Tech Publ, Switzerland, 1984.
- [16] W.L. Johnson, A. Inoue, C.T. Liu, (Eds.), *Bulk Metallic Glasses*, MRS Symposium Proceedings, Vol. 554, Materials Research Society, Warrendale, PA, 1999.
- [17] R. Busch, *JOM* 52 (7) (2000) 39.
- [18] A.R. Yavari, A. Inoue, in: W.L. Johnson, A. Inoue, C.T. Liu (Eds.), *Bulk Metallic Glasses*, MRS Symposium Proceedings, Vol. 554, Materials Research Society, Warrendale, PA, 1999, p. 21.
- [19] A.V. Granato, *Phys. Rev. Lett.* 68 (1992) 974.
- [20] P.R. Okamoto, N.Q. Lam, L.E. Rehn, in: H. Enrenreich, F. Spaepen (Eds.), *Solid State Physics*, vol. 52, Academic Press, San Diego, 1999, p. 1.
- [21] M. Winter, *WebElements™ Periodic Table*, Professional Edition, <http://www.webelements.com>, University of Sheffield, UK, 2000.
- [22] J.L.C. Daams, P. Villars, J.H.N. van Vucht, *Atlas of Crystal Structure Types for Intermetallic Phases*, vol. 1–4, ASM International, Materials Park, OH, 1991.
- [23] *International Tables for X-Ray Crystallography*, Birmingham, England, 1968.